Journal of Medicinal Chemistry

Brief Article

Synthesis and Biological Evaluation of Vitamin D3 Metabolite 20*S*,23*S*-Dihydroxyvitamin D3 and Its 23*R* Epimer

Zongtao Lin, Srinivasa R. Marepally, Dejian Ma, Tae-Kang Kim, Allen SW. Oak, Linda K Myers, Robert C. Tuckey, Andrzej T. Slominski, Duane D Miller, and Wei Li

J. Med. Chem., **Just Accepted Manuscript** • DOI: 10.1021/acs.jmedchem.6b00182 • Publication Date (Web): 12 Apr 2016

ACS Publications

Journal of Medicinal Chemistry is published by the American Chemical Society. 1155 Sixteenth Street N.W., Washington, DC 20036

Synthesis and Biological Evaluation of Vitamin D3 Metabolite 20*S*,23*S*-Dihydroxyvitamin D3 and Its 23*R* Epimer

Zongtao Lin[†], Srinivasa R. Marepally[†], Dejian Ma[†], Tae-Kang Kim[‡], Allen SW. Oak[‡], Linda K. Myers[¶], Robert C. Tuckey[§], Andrzej T. Slominski[‡,‖], Duane D. Miller[†], Wei Li[*,†]

†. Department of Pharmaceutical Sciences, University of Tennessee Health Science Center, Memphis, TN 38163, United States.

‡. Department of Dermatology, University of Alabama at Birmingham, VA Medical Center, AL 35294, United States.

¶. Department of Medicine, University of Tennessee Health Science Center, Memphis, TN 38163, United States.

§. School of Chemistry and Biochemistry, University of Western Australia, Crawley, WA 6009, Australia.

‖. VA Medical Center at Birmingham, Birmingham, AL 35294, United States.

KEYWORDS. 20,23-dihydroxyvitamin D3; LAIR1; CYP11A1; CYP27B1; metabolism; vitamin D receptor.

ABSTRACT: The vitamin D3 metabolite, 20*S*,23*S*-dihydroxyvitamin D3, was chemically synthesized for the first time, and identified to be the same as the enzymatically produced metabolite. The C23 absolute configurations of both 20*S*,23*S*/*R*-dihydroxyvitamin D3 epimers were unambiguously assigned by NMR and Mosher ester analysis. Their kinetics of CYP27B1 metabolism were investigated during the production of their 1α-hydroxylated derivatives. Bioactivities of these products were compared in terms of vitamin D3 receptor activation, anti-inflammatory and anti-proliferative activities.

INTRODUCTION

The classical pathway for metabolism (**Figure 1**) of vitamin D3 (VD3) starts with hydroxylation at C25 by microsomal cytochrome P450 enzyme, CYP2R1[1] or the mitochondrial CYP27A1[2], producing 25-hydroxyvitamin D3 [25(OH)D3], primarily in the liver. 25(OH)D3 then undergoes 1α-hydroxylation in the kidney by CYP27B1 producing the active form of vitamin D3, 1α,25-dihydroxyvitamin D3 [1,25(OH)$_2$D3]. Inactivation of 1,25(OH)$_2$D3 mainly involves CYP24A1-catalyzed hydroxylation and oxidation, ultimately producing calcitroic acid for excretion[3, 4].

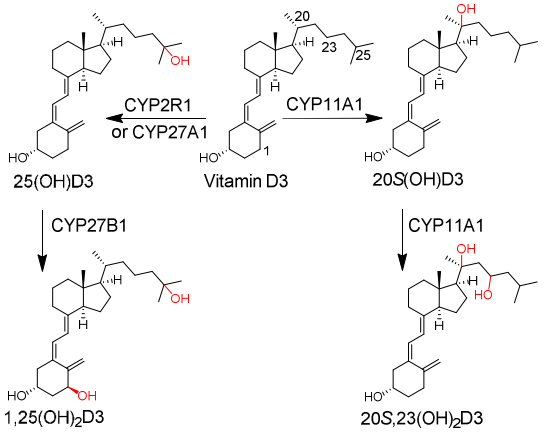

Figure 1. VD3 is metabolized to 25(OH)D3 and 1,25(OH)$_2$D3 by the classical pathway or to 20*S*(OH)D3 and 20*S*,23(OH)$_2$D3 by CYP11A1.

An alternatively novel pathway of VD3 metabolism is initiated by CYP11A1[5-8]. CYP11A1 can metabolize VD3 into several mono-, di- and tri-hydroxylated bioactive metabolites, with 20*S*-hydroxyvitamin D3 [20*S*(OH)D3] and 20*S*,23-dihydroxyvitamin D3 [20*S*,23(OH)2D3] being the most comprehensively studied so far[9]. These two metabolites were initially produced enzymatically *in vitro* by incubating VD3 with bovine CYP11A1[5, 6]. Subsequent investigations detected the formation of these metabolites from VD3 in keratinocytes, adrenal glands, and human placenta, indicating the occurrence of these CYP11A1-mediated pathways in these cells or tissues[7-9]. Final proof on the occurrence of this pathway *in vivo* was detection of 20*S*(OH)D3, 20*S*,23(OH)2D3 and related hydroxy derivatives in the human epidermis and serum[10]. Interestingly, the epidermal levels of 20*S*(OH)D3 and 22(OH)D3 were higher than that of 25(OH)D3, but lower in the serum, however, at levels above those required for biological activity as measured *in vitro*[10].

The biological activities of 20*S*(OH)D3 and 20*S*,23(OH)$_2$D3 have been demonstrated in a large number of *in vitro* and *in vivo* systems[9, 11, 12]. They are biased agonists of the vitamin D receptor (VDR) and share many but not all biological actions of 1,25(OH)$_2$D3[9, 11, 12]. Both of them are inverse agonists on RORα and RORγ[13]. They inhibited the proliferation and stimulated differentiation of epidermal keratinocytes and leukemia cells from human and mouse[14, 15], and showed anti-melanoma activity[11, 16]. In addition, 20*S*(OH)D3 and 20*S*,23(OH)$_2$D3 exerted their anti-inflammatory activities through downregulation of NFκB activity in normal and immortalized keratinocytes[17-19], and displayed anti-fibrotic effects on human dermal fibroblasts from scleroderma patients and anti-fibrotic activity in animal models[20]. 1,25(OH)$_2$D3 is a strong inducer of CYP24A1 which catalyzes the inactivation of vitamin D metabolites[21], whereas 20*S*(OH)D3 and 20*S*,23(OH)$_2$D3 are poor stimulators of CYP24A1 expression, suggesting they are less prone to rapid metabolism by this enzyme[9]. Moreover, while 1,25(OH)$_2$D3 causes hypercalcemia in rats and mice, both 20*S*(OH)D3 and 20*S*,23(OH)$_2$D3 are non-calcemic at much higher doses (up to 30 μg/kg in mice)[15, 22]. Thus 20*S*(OH)D3 and 20*S*,23(OH)$_2$D3 have great potential for further development as adjuvant therapeutic agents, especially for a wide variety of immune-driven diseases.

While the structure of enzymatically produced 20*S*,23(OH)$_2$D3 has been elucidated by NMR analysis[6], the absolute configuration at C23 has not been determined unambiguously due to the limited amount of material available. It is well known that the

absolute configuration of molecules can have substantial impacts on their biological activities. Therefore, the aim of this study was to: (1) synthesize both epimers of 20*S*,23*R*/*S*(OH)2D3 chemically and determine their absolute configurations by NMR and Mosher ester analyses; (2) identify which epimer corresponds to the enzymatically generated, biologically active 20*S*,23(OH)2D3 metabolite by using HPLC and NMR; (3) evaluate the ability of CYP27B1 to metabolize these two epimers for the production of their 1α-OH derivatives; and (4) assess the differential biological activities for these two epimers as well their 1α-OH derivatives with respect to VDR activation, antiproliferative and anti-inflammatory effects.

Scheme 1. Synthesis of compounds 17 and 18[a]

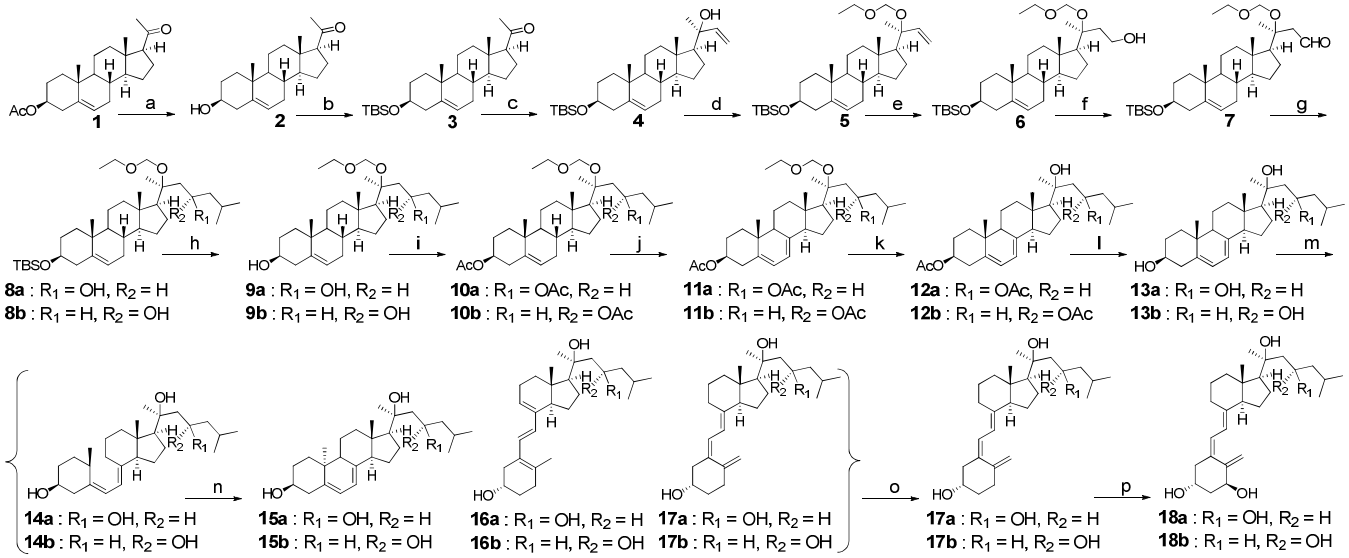

[a]Reagents and conditions: (a) aq. KOH, MeOH, r.t., 2 h. 94%. (b) TBSCl, imidazole, DMF, r.t., overnight. 92%. (c) Vinylmagnesium bromide, THF, 0 ºC - r.t., overnight. 84%. (d) EOMCl, DIPEA, CH_2Cl_2, r.t., overnight. 92%. (e) 9-BBN, THF, 0 ºC - r.t., 24 h; H_2O, r.t., 0.5 h; NaOH, H_2O_2, -20 ºC - r.t., overnight. 81%. (f) PDC, CH_2Cl_2, r.t., 24 h. 96%. (g) Isobutyl bromide, Mg, THF, I_2, 45 ºC, 1 h; THF, 0 ºC - r.t., 6 h. 85%. (h) TBAF, THF, r.t., 12 h. 100%. (i) Ac_2O, pyridine, DMAP, 12 h. 94%. (j) Dibromantin, AIBN, Benzene: Hexane (1:1), reflux 20 min; TBAB, THF, r.t., 75 min, then TBAF, r.t., 50 min. 39%. (k) Mont. K10, ACN, 0 ºC - r.t., 12 h. 65% (35% recovered). (l) aq. KOH, MeOH, 2 h. 85%. (m) UVB, Et_2O, 15 min. (n) Ethanol, reflux, 3 h. (o) HPLC, ACN:H_2O. 11% (three steps). Overall yield from step (a) to (o) is 1.5%. (p) CYP27B1 enzyme.

RESULTS AND DISCUSSION

Chemistry. The synthetic route to make 20*S*,23*R*(OH)$_2$D3 and 20*S*,23*S*(OH)$_2$D3 is shown in **Scheme 1**. Detailed synthesis procedures and structural characterizations of intermediates and products are listed in the **supporting information**. Briefly, the 3-acetyl on commercially available pregnenolone acetate (**1**) was first replaced by TBS protection after deacetylation under basic condition[23]. This replacement allowed 3-OTBS to go through later Grignard reactions and hydroboration safely and intact. Addition of vinyl magnesium bromide to 20-ketone (**3**) afforded alcohol **4** with a stereospecific 20*S* configuration as reported in our previous studies[21, 24, 25]. The 20-OH was then protected by EOMCl and excess DIPEA in DCM with satisfactory yield (92%). Intermediate **6** was obtained by 9-BBN hydroboration, and went through PDC oxidation to give aldehyde **7**, in which the aldehyde group was utilized to react with isobutylmagnesium bromide to produce two epimers (**8a** and **8b**) with different C23 configuration. Our initial trials to separate **8a** and **8b** using different solvent systems for normal phase TLC failed to obtain pure diastereomers. Fortunately, after being treated with TBAF, mixture **8** gave two separated spots (alcohols **9a** and **9b**) on TLC which were further separated using flash column chromatography for the following reactions. Di-acetylation of 3-OH and 23-OH on **9** afforded protected **10**, which was subsequently transformed into the 5,7-diene 7DHC structure (**11**) by a well-established procedure using dibromantin/AIBN/TBAB/TBAF conditions[26]. EOM protection on C20 was removed to keep the configurations of 3-OH and 23-OH unaffected. In this study, montmorillonite K10 clay was found to be a neat catalyst for the removal of EOM protection at room temperature. Hydrolysis of ester bonds under KOH/MeOH condition rapidly yielded the 7DHC structure (**13**). To get secosteroid structures, B-ring-opening reaction using UVB light irradiation was carried out for **13** dissolved in ethyl ether, followed by heat induced isomerization of pre-vitamin D3 to produce VD3 product (**17a** as isomer I or **17b** as isomer II). Normal phase LC was unable to separate **17** out of the reaction mixture, so HPLC was used for the purification of **17** using acetonitrile (ACN) and water as mobile phases. 1α-Hydroxylated product **18** was produced by enzymatic reaction with CYP27B1 which is highly specific for the 1α-position based on its function[27], and was purified by HPLC.

Isomer II (17b) showed matched retention times with the CYP11A1 product in HPLC chromatograms. To determine which one of the chemically synthesized 20*S*,23(OH)$_2$D3 epimers is identical to the CYP11A1 product, HPLC analysis was carried out to compare their chromatographic behaviors. As shown in **Figure 2**, isomer II under different reverse phase HPLC conditions (methanol: water for A and B, and acetonitrile: water for C and D) gave the same retention times as that of enzymatically produced 20*S*,23(OH)$_2$D3, strongly suggesting that isomer II has the same structure as the natural metabolite discovered previously[6, 14].

In addition, our previous study has elucidated the structure of enzymatic 20*S*,23(OH)$_2$D3, and the NMR and UV spectra of synthetic **17b** further confirmed that it was identical to the reported

natural product. For comparison, the spectra of **17a** and **17b** are listed in **supporting information** (**Figure S22-30** for spectra and **Table S2** for proton NMR chemical shift assignments). High-resolution MS spectra obtained using a Waters UPLC coupled to a Xevo G2-S qTof MS system also confirmed their identical structures, using an optimized method[28, 29].

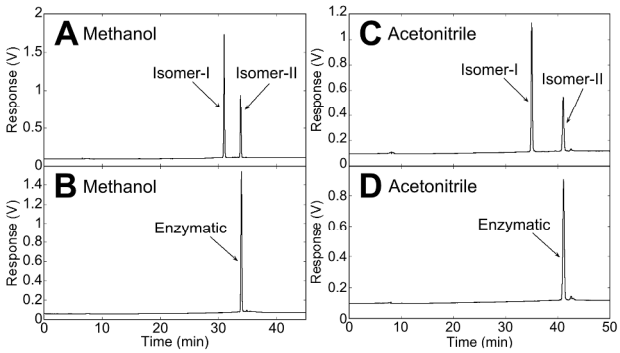

Figure 2. Comparison of HPLC retention times of 20*S*,23(OH)$_2$D3 isomers produced chemically and enzymatically. Chemically synthesized isomer I (2 nmol) and isomer II (1 nmol) were combined (A and C) and analyzed by HPLC in comparison to 2 nmol enzymatically synthesized 20*S*,23(OH)$_2$D3 (B and D). Isomer II (17b) was found to be the enzymatically produced isomer.

Identification of 9a having a 23*R* configuration and 9b having a 23*S* configuration by NMR. To determine the C23 configurations of isomer I (**17a**) and isomer II (**17b**), intermediates **9a** and **9b** maintaining the same C23 configurations with **17a** and **17b** were used. Their NMR (1D and 2D) spectra were recorded and compared to assign their C23 configurations with assistance of molecular modeling. Their HSQC, HMBC and NOESY spectra are shown in **Figure 3** and **S1-13**. The assignments of their ^{1}H and ^{13}C chemical shifts are listed in **Table S1**. Six methyl signals belonging to the ring system (18-, 19-, 21-, 26- and 27-methyls) and one from EOM protection, CH groups and CH$_2$ groups were all identified on HSQC (**Figure S11**). All four quaternary carbons (C5, C10, C13 and C20) were assigned based on their HMBC spectra (**Figure S12**). The assignment strategy is similar to that of previously reported di- and tri-hydroxyvitamin D3 metabolites[6, 24].

Distances used to distinguish the two epimers are shown in **Figure 3**. NOE integrals of 6H to 7H$_\beta$ and to 4H$_\alpha$ were used as internal references to calibrate other NOE peak integrals (**Figure S13**). The NOE integrals of reference protons in **9a** and **9b** are comparable as seen in the middle panels of **Figure 3B** and **3C** (or **Figure S13**); however, the NOE peak integral of 23H to the centroid of 21-CH$_3$ in **9a** (left panel of **Figure 3B**) is 2.5 times smaller than that in **9b** (left panel of **Figure 3C**). Based on the internal reference distances, the calculated distance between 23H and the centroid of 21-CH$_3$ in **9a** (3.94 Å) is larger than that in **9b** (2.98 Å) (**Figure 3A**). Based on the modelling structures incorporating these NOE distance constraints, we tentatively conclude that **9a** and **9b** have 23*R* and 23*S* configurations, respectively.

Further NMR evidence for the C23 stereochemistry of **9a** and **9b** is provided by the chemical shifts of neighboring C22 protons as shown in the right panels of **Figure 3B** and **3C**. In the 23*R* (**9a**) modeled structure, 23-O and 20-O are oriented towards opposite directions, while they are oriented towards similar directions in the 23*S* (**9b**) configuration (**Figure 3A**). Consequently, the two germinal protons at C22 experience a relatively similar chemical environment in 23*R* (**9a**) and a very different chemical environment in 23*S* (**9b**). The related distances are shown in **Figure 3A**. The two C22 germinal protons showed a similar chemical shift (both are at 1.68 ppm) in **9a**, but very different chemical shifts (1.92 and 1.58 ppm) in **9b** (**Table S1**). Therefore, the chemical shift patterns of the two protons in 22-CH$_2$ also suggest that the 23 configuration of **9a** is *R*, and **9b** is *S*.

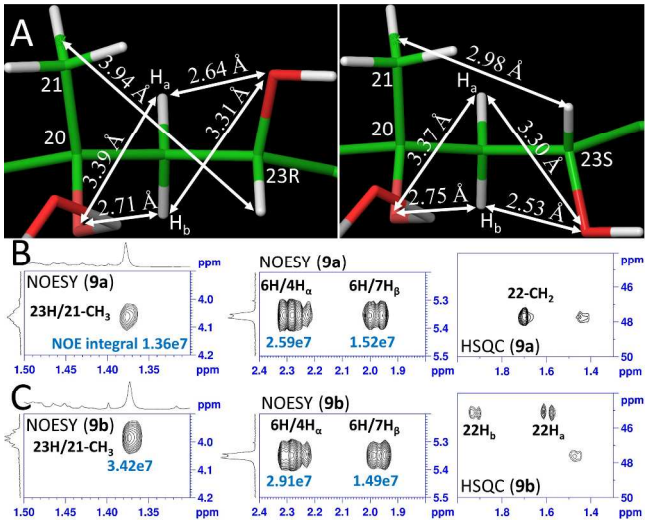

Figure 3. Molecular models (A) after energy minimization and the 2D NMR for 9a (23*R*) (B) and 9b (23*S*) (C). The distance (3.94 Å) between 23H and the centroid of 21-CH$_3$ in the 23*R*-configuration is longer than that of the 23*S*-configuration based on their NOE peak integrals. The chemical environments for 22H$_a$ and 22H$_b$ are affected by 23-O and 20-O symmetrically in the 23*R*-configuration, and thus they have similar chemical shifts. In contrast, these two protons are in different environments created by the 23-O and 20-O in 23*S*-configuration, and thus have very different chemical shifts.

Confirmation of the 23*R* configuration of 9a by Mosher ester analysis. To confirm our tentative assignments that **9a** has a 23*R* configuration based on the above NMR analysis, we performed the Mosher ester analysis for **9a**. In this intermediate, there are two free OH groups, and two reactions were carried out by transforming **9a** to *S*- and *R*-Mosher 3,23-di-esters, separately (**Scheme 2**). The 3-OH has a known β position which makes C3 an *S* configuration, 3*S* is thus used as an internal reference. The ^{1}H-NMR, ^{1}H-^{1}H COSY and ^{19}F-NMR spectra of *S*- and *R*-Mosher esters of **9a** are shown in **Figure S14-19**. The ^{1}H chemical shifts of 2-CH$_2$ and 4-CH$_2$ were used to verify the 3*S* configuration, and the ^{1}H chemical shifts of 22-CH$_2$ and 24-CH$_2$ were used to determine the C23 configuration. The results of Mosher ester analysis are shown in **Table 1**. C23 of **9a** was unambiguously identified as 23*R* according to the chemical shifts of 22-CH$_2$ and 24-CH$_2$ in the *S*- and *R*-Mosher esters, **9b** was thus assigned as 23*S*. Since **17a** and **17b** were produced from **9a** and **9b** separately with intact C23 configurations, they were assigned as 20*S*,23*R*(OH)$_2$D3 and 20*S*,23*S*(OH)$_2$D3, respectively. This assignment is consistent with the NMR analyses described earlier.

Scheme 2. Synthesis of Mosher esters 19a and 19b[a]

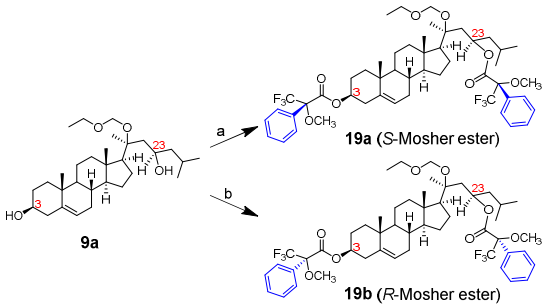

[a]Reagents and conditions: (a) (*R*)-Mosher acid chloride, Et_3N, DMAP, DCM, r.t., overnight, 80%. (b) (*S*)-Mosher acid chloride, Et_3N, DMAP, DCM, r.t., overnight, 88%.

Table 1. ^{1}H-NMR chemical shifts of 9a, *S*- and *R*-Mosher esters ($\Delta\delta = \delta S - \delta R$). The C3-configuration was used as an internal standard. Chemical shifts of Mosher esters were assigned from ^{1}H-^{1}H COSY spectra.

	^{1}H-NMR chemical shift (ppm)					
	$2H_\alpha$	$2H_\beta$	4-CH_2	22-CH_2	24H'	24H"
9a	1.84	1.51	2.26	1.68	1.43	1.10
19a (*S*-ester)	1.91	1.61	2.46	1.92	1.63	1.48
19b (*R*-ester)	1.98	1.73	2.36	1.96	1.58	1.44
$\Delta\delta$	-0.07	-0.08	0.10	-0.04	0.05	0.04
	C3 of **9a** is *S*			C23 of **9a** is *R*		

Kinetics of the metabolism of 20*S*,23*R*(OH)$_2$D3 (17a) and 20*S*,23*S*(OH)$_2$D3 (17b) by mouse CYP27B1. CYP27B1 plays a key role in the activation of 25(OH)D3 to 1,25(OH)$_2$D3 and can also 1α-hydroxylate 20*S*,23(OH)$_2$D3 which alters its biological properties[4, 30, 31]. We therefore compared the abilities of mouse CYP27B1 to hydroxylate **17a** and **17b** (**Table 2**). CYP27B1 specifically adds a 1α-OH group to a range of VD3 analogs including 25(OH)D3, 20*S*(OH)D3, 20*S*,24*R*(OH)$_2$D3 and 20*S*,24*S*(OH)$_2$D3 [4, 24, 27, 30, 31]. Using well established procedures[30, 31], **17b** was converted to **18b** by CYP27B1, as further confirmed by using an authentic, enzymatically produced standard[27]. **17a** was presumably metabolized into its 1α-hydroxylated product based on the hydroxylation specificity of CYP27B1 for this position[4, 31]. **17a** displayed both K_m and K_{cat} values half those for **17b**, therefore the overall catalytic efficiency (K_{cat}/K_m) of CYP27B1 for metabolism of these two epimers is approximately the same. However, the higher K_{cat} value for **17b** indicates that CYP27B1 has a higher capacity to hydroxylate this compound than its unnatural epimer having a 23*R*-configuration when substrate concentrations are high.

Table 2. Kinetics of the metabolism of 20*S*,23*R*(OH)$_2$D3 and 17b by CYP27B1.[a]

Substrate	K_m	K_{cat}	K_{cat}/K_m
20*S*,23*R*(OH)$_2$D3 (**17a**)	2.3 ± 0.8	1.17 ± 0.08	5087
20*S*,23*S*(OH)$_2$D3 (**17b**)	5.2 ± 1.8	2.46 ± 0.22	4731

[a] K_m, 10^{-3} mol/mol phospholipid (PL); K_{cat}, min^{-1}; K_{cat}/K_m, min^{-1}(mmol/mol PL)$^{-1}$.

The abilities of 20*S*,23*R*(OH)$_2$D3, 20*S*,23*S*(OH)$_2$D3 and their 1α-OH derivatives to activate the VDR. The VDR is known to mediate many activities of vitamin D compounds, and has been shown to be required for the stimulation of differentiation and CYP24A1 expression in keratinocytes by enzymatically produced **17b**[18]. To test the differential abilities of **17a** and **17b** together with their 1α-hydroxylated derivatives, to activate the VDR, a synthetic VDR transcriptional promoter (VDRE) was transduced into three different cell lines previously used for a lentiviral VDRE-luciferase reporter assay[21, 24]. The three cell lines used were HaCaT cells as a model of normal human keratinocyte, Caco-2 cells as a cancer cell model and Jurkat cells as an immune cell model. Two well-known VDR agonists, 1,25(OH)$_2$D3 and 22-oxa-1,25(OH)$_2$D3, were used as positive controls in this assay. Both of them showed low EC50 values for VDR activation using the luciferase reporter assay in all three cell lines (**Table 3**), with 22-oxa-1,25(OH)$_2$D3 being more potent than 1,25(OH)$_2$D3. In particular, they gave low nM EC50s in Jurkat cells, suggesting their selectivity among different cell types. Importantly, **17b** was unable to activate VDR at a concentration up to 1,000 nM, while **17a** showed a strong stimulatory effect at this concentration in all three cell lines, indicating that the 23*R* configuration favors VDR activation with the synthetic VDRE used, compared to the 23*S* epimer. Both 1α-OH derivatives (**18a** and **18b**) were more potent than their parent compounds, consistent with 1α-hydroxylation causing activation, as for 25(OH)D3[4, 27]. Molecular modeling also suggests increased binding interactions of the 1α-OH derivatives (**18a** and **18b**) to the VDR than for **17a** and **17b** (**Figure S32**). Similarly, **18a** with a 23*R* configuration showed a lower EC50 value than **18b** with a 23*S* configuration, particularly in Jurkat cells, which is consistent with the relative potencies of **17a** and **17b** (parent compounds).

Upregulation of LAIR1 levels as a marker of anti-inflammatory activity. Leukocyte-associated immunoglobulin-like receptor 1 (LAIR1), also called CD305 (cluster of differentiation 305), is an inhibitory receptor expressed in peripheral mononuclear cells including natural killer cells, T cells and B cells in the immune system[32]. This inhibitory receptor downregulates immune responses and prevents cell lysis, thus it is recognized as an anti-inflammatory protein marker in autoimmunity[32]. Previously, we reported that 20*S*,24*S*/*R*(OH)$_2$D3 and their 1αOH-derivatives upregulate the concentration of LAIR1, indicating their anti-inflammatory effects[24]. To test whether 20*S*,23*S*/*R*(OH)$_2$D3 and their 1αOH-derivatives also possess anti-inflammatory activities, we measured LAIR1 levels by flow cytometry in mice splenocytes following treatment with these secosteroids. **Table 3** shows that all these compounds including the two positive controls significantly elevated the level of LAIR1 at a concentration of 100 nM. **17a**, **17b**, **18a** and **18b** showed increases comparable with that of 22-oxa-1,25(OH)$_2$D3, and these effects were stronger than that of 1,25(OH)$_2$D3. In addition, **18a** and **18b** showed similar stimulatory effects to their parent compounds (**17a** and **17b**), indicating that 1α-hydroxylation is not necessary for the anti-inflammatory activity of these secosteroids. These finding are consistent with previously reported inhibitory effects of 20*S*(OH)D3 and 20*S*,23(OH)D3 on production of pro-inflammatory cytokines by mouse and human lymphocytes[9, 13].

Finally, we tested the anti-proliferative activity of these compounds on SKMEL-188 melanoma cells (**Figure S33**). All D3 derivatives moderately inhibited growth of melanoma cells at concentrations of 0.1-1.0 nM in a dose dependent manner, similar to the classical 1,25(OH)$_2$D3 (the effect was statistically significant). The IC_{50} values ranged from 10^{-11} to 10^{-10} M being similar for the 20,23(OH)$_2$D3 isomers, their 1αOH-derivatives (**18a** and **18b) and** 1,25(OH)$_2$D3. However, **18a** and **18b** showed higher maximal inhibition values (**Figure S33**) suggesting that addition of a 1αOH can potentiate the antiproliferative effect.

Table 3. Biological activities of 20*S*,23*R*(OH)$_2$D3, 20*S*,23*S*(OH)$_2$D3 and their 1α-OH derivatives compared to 1,25(OH)$_2$D3 and 22-oxa-1,25(OH)$_2$D3. [a]

Compound	VDRE activation (EC50, nM)			LAIR1 level (MF, AU)
	HaCaT	Caco-2	Jurkat	
Vehicle control	NA	NA	NA	766 ± 22
20*S*,23*R*(OH)$_2$D3 (**17a**)	484 ± 28	562 ± 34	653 ± 61	1481 ± 24
20*S*,23*S*(OH)$_2$D3 (**17b**)	NS	NS	NS	1479 ± 98
1α,20*S*,23*R*(OH)$_3$D3 (**18a**)	116.9 ± 0.21	171.7 ± 3.4	30.64 ± 0.39	1478 ± 78
1α,20*S*,23*S*(OH)$_3$D3 (**18b**)	174.8 ± 8.2	241.4 ± 10	203.0 ± 12.9	1480 ± 53
1,25(OH)$_2$D3	249.7 ± 1.8	223.4 ± 0.8	3.936 ± 0.070	1355 ± 28
22-oxa-1,25(OH)$_2$D3	159.7 ± 3.4	144.5 ± 3.0	0.855 ± 0.036	1479 ± 72

[a] **NA: not applicable. NS: no significance. MF: mean fluorescence. LAIR1 levels were measured at 100 nM of compound.**

In this study, the bioactive VD3 metabolite 20*S*,23*S*(OH)$_2$D3 (**17b**) and its non-natural epimer 20*S*,23*R*(OH)$_2$D3 (**17a**) were chemically synthesized, and their C23 configurations were unambiguously assigned by NMR and Mosher ester analyses. **17b** was identified as the enzymatic product of VD3 metabolism by CYP11A1[6] by HPLC and NMR. Comparison of the kinetics of **17a** and **17b** metabolism by CYP27B1 showed that they have similar catalytic efficiencies for 1α-hydroxylation. This enzymatic 1α-hydroxylation was exploited to make small quantities of **18a** and **18b** for analyzing the effect of the 1α-hydroxyl group on biological activity. Using a synthetic VDRE construct and a luciferase reporter assay we observed that **17a**, but not **17b**, could cause VDR activation. The modest activation of the VDRE by **17a** is consistent with low activation of VDRE of CYP24A1 promoter in our previous study in keratinocytes and leukemia cells, where involvement of the VDR was demonstrated[11, 18]. This is also consistent with our assessment that these compounds act as biased agonists on VDR signaling system[9, 11, 12], and that their biological activity also involves RORs[13]. Both epimers caused VDRE transcriptional activation following 1α-hydroxylation, with the 23*R* epimer being more potent. These results are consistent with our previous observations on the relative potencies of 20*S*,24*R*/*S*(OH)$_2$D3[24]. 23*R*- and 23*S*-epimers, 1α-hydroxylated or not, showed somewhat different potencies in all three cell lines tested, suggesting an enhanced interaction with the VDR/VDRE complex in immune cells, possibly due to high expression of the VDR or high concentrations of specific coactivators in immune cells that mediate the VDR responses, compared to the other cells tested[4]. Interestingly, the EC50 for **18a** in Jurkat cells was six times lower than that of **18b**. Analysis of the docking of these compounds using the VDR crystal structure, further correlated their potencies to their binding interactions with the VDR, with 1α-hydroxylation markedly increasing the docking score. The anti-inflammatory potential of the C23 epimers was assessed by their ability to increase LAIR1 levels and their anti-proliferative ability from the MTS assay which measures mitochondrial activity. Results reveal that the C23 epimers, both with and without a 1α-hydroxyl group, have potent anti-inflammatory and anti-proliferative activities, better or at least comparable with that of 1,25(OH)$_2$D3 and/or 22-oxa. The lack of a requirement for 1α-hydroxylation for the anti-inflammatory activity of the novel secosteroids is consistent with the recent discovery that they act as inverse agonists on RORγ, a driver of proinflammatory responses[13]. In contrast, addition of a 1αOH group to the novel secosteroids can increase their affinity towards the VDR[12] leading to improved anti-proliferative activity[9]. The exact mechanisms and structural requirements for these different biological activities remain to be elucidated with further in-depth mechanistic studies.

CONCLUSION

In summary, 20*S*,23*R*/*S*(OH)$_2$D3 (**17a**/**17b**) and their 1α-OH metabolites (**18a**/**18b**) were synthesized for the first time, and 20*S*,23*S*(OH)$_2$D3 (**17b**) was confirmed to be the natural metabolite. These compounds showed different abilities to activate the VDR with **18a** being the most potent. They all showed anti-inflammatory and anti-proliferative activities, although these different biological activities were not linearly correlated, most likely due to distinct mechanisms and structural requirements leading to these biological activities. Further biological studies of the unnatural metabolite, **18a**, will be necessary to investigate its drug-like properties in comparison to its natural 23*S* counterpart.

EXPERIMENTAL SECTION

General procedures. See **supporting information** for chemistry procedures of intermediates and final products.

HPLC. Purities (**Figure S28-29**) of final VD3 products (**17a** and **17b**) were determined by using an Agilent HPLC 1100 system and a Phenomenex Luna-PFP C18 column (5 μm, 250 mm × 4.6 mm, Torrance, CA) at 25°C and a flow rate of 1.0 mL/min. Acetonitrile and water were used as mobile phases with a gradient comprising 40-70% acetonitrile for 30 min. 263 nm was used to display chromatograms. The purities of **17a** and **17b** were determined as ≥98%.

For identifying which chemically synthesized product was identical to enzymatic product by HPLC, retention times of chemically synthesized isomer I (**17a**) and isomer II (**17b**) were compared with that of enzymatic 20*S*,23(OH)$_2$D3. HPLC was carried out on a C18 column (Grace Alltima, 25 cm × 4.6 mm, 5 μm) with secosteroids being monitored by a UV detector at 265 nm. Two different solvent systems were used, 64 – 100% methanol for 20 min, then 100% methanol for 25 min or 45 – 100% acetonitrile for 25 min, then 100% acetonitrile for 25 min. The flow rate was 0.5 mL/min.

NMR. All NMR data were collected on a Bruker Avance III 400 MHz NMR (Bruker BioSpin, Billerica, MA). Samples were dissolved in 0.5 mL $CDCl_3$ and NMR data were collected at room temperature. TMS was used as an internal standard.

Metabolism of the C23 epimers by CYP27B1. To measure the kinetics of **17a** and **17b** metabolism by CYP27B1, substrate was

incorporated into phospholipid (PL) vesicles at a range of concentrations (0.0025 – 0.07 mol/mol PL)[24, 30, 31]. The amount of product after a 3 min incubation with 0.1 μM mouse CYP27B1 was determined by HPLC[30]. Kinetic parameters were determined by fitting the Michaelis-Menten equation to the data with Kaleidagaph 4.1.1. Data for K_m and K_{cat} are presented as mean ± standard error of the curve fit. This procedure was scaled up and the incubation time extended to 1 h to produce μg amounts of the 1α-hydroxy derivatives for biological testing, as described before[30, 31]. After incubation, the product (**18a** or **18b**) was extracted with dichloromethane, dried, and purified by HPLC on a C18 column (Grace Alltima, 25 cm × 4.6 mm, 5 μm) using an acetonitrile in water gradient at a flow rate of 0.5 mL/min: 45 – 100% acetonitrile for 25 min then 100% acetonitrile for 25 min. The two epimers were further purified on the same column using a methanol gradient: 46 - 100% methanol for 15 min then 100% methanol for 25 min, at 0.5 mL/min.

Cell cultures. HaCat, Caco-2 and Jurkat cells were transduced with a lentiviral VDRE-luciferase reporter vector as before[21, 24]. Cells were grown in media as follows. Caco-2 cells: Dulbecco's Modified Eagle Medium (DMEM) supplemented with 10% fetal bovine serum (FBS) and 1% penicillin/streptomycin/amphotericin antibiotic solution (Ab) (Sigma-Aldrich, St. Louis, MO). HaCaT cells: The same medium used for caco-2 cells with 10% FBS changed into 5% FBS. Jurkat cells: RPMI 1640 medium supplemented with 10% FBS and 1% Ab. Splenocytes from mice: Eagles Minimal Essential Medium (EMEM) supplemented with 9% charcoal-stripped FBS, 100 U/mL penicillin and 100 μg/mL streptomycin, non-essential amino acids, 2.5 mM 2-mercaptoethanol and 2.5 mM *L*-glutamine. SKMEL-188 melanoma cells: Ham's F10 medium supplemented with 5% FBS and 1% Ab. All cells were cultured at 37 °C in a humidified atmosphere containing 5% CO_2.

VDRE-luciferase transcriptional reporter assay. HaCaT, Caco-2 and Jurkat cells were selected for one week by culturing in medium containing additional 1.0 μg/mL puromycin. Each cell line was then plated in a 96-well plate (10,000 cells/well, 100 μL medium) using FBS-free media and incubated for 24 h to synchronize the cells. Secosteroids at a series of concentrations were added separately to 96-well plate (1.0 μL/well). The final concentration of DMSO was 0.1%. Cells were incubated for another 24 h, and then 100 μL solution of ONE-Glo™ Luciferase Assay System (Promega, Madison, WI) was added to each well. After 5 min reaction at room temperature, the luciferase signal was detected by a BioTek Synergy HT microplate reader (BioTek Instruments, Inc., Winooski, VT, US). All concentrations of secosteroids were tested in triplicate.

Measurement of LAIR1 concentrations by Flow cytometry. Splenocytes isolated from DBA/1 mice were used to measure the LAIR1 levels. The cells were treated with each secosteroid at a concentration of 10^{-7} M, ethanol was used as vehicle control. After overnight incubation, cells were labeled with specific fluorochrome antibodies for both CD_4 (BD Biosciences, San Jose, CA) and LAIR1 (eBioscience, San Diego, CA). The LAIR1 level was then determined by flow cytometry (multi-parameter) using an LSRII flow cytometer (BD Biosciences, San Jose, CA) when gating was performed on CD_4 cells. At least 10,000 cells were analyzed from each sample. Final results were obtained from Flow software (Tree Star, Ashland, OR) analysis. Results are expressed as the mean of quadruplicate values ± standard error (*n* = 4).

ASSOCIATED CONTENT

Supporting Information.
Preparation and characterization of compounds.

AUTHOR INFORMATION

Corresponding Author

*Phone: +1 (901) 448 7532. Fax: +1 (901) 448 6828. E-mail: wli@uthsc.edu. Address: 881 Madison Avenue, Room 561, Memphis, TN 38163, United States.

Notes

The authors declare no competing financial interest.

AKNOWLEDGEMENTS

This work was supported by NIH grants 1R21AR063242 (W.L. and D.D.M.), 1S10OD010678 (W.L.), 1S10RR026377 (W.L.), 2R01AR052190 (A.S.), 1R01AR056666-01A2 (A.S.) and R21AR066505 (A.S.). The content is solely the responsibility of the authors and does not necessarily represent the official views of the NIH.

ABBREVIATIONS

$1,25(OH)_2D_3$, 1α,25-dihydroxyvitamin D_3; 20*S*(OH)D_3, 20*S*-hydroxyvitamin D_3; 20*S*,23$(OH)_2D_3$, 20*S*,23-dihydroxyvitamin D_3; 22-oxa, 22-oxa-1α,25-dihydroxyvitamin D_3; 25(OH)D_3, 25-hydroxyvitamin D_3; 7DHC, 7-dehydrocholesterol; 9-BBN, 9-Borabicyclo[3.3.1]nonane; ACN, acetonitrile; AIBN, azobisisobutyronitrile; COSY, ^1H-^1H correlation spectroscopy; CYP, cytochrome P450 enzyme; DIPEA, diisopropylethylamine; DMF, dimethylformamide; DMAP, 4-dimethylaminopyridine; EOMCl, chloromethyl ethyl ether; HMBC, ^1H-^{13}C heteronuclear multiple bond correlation spectroscopy; HSQC, ^1H-^{13}C heteronuclear single quantum correlation spectroscopy; LAIR1, leukocyte-associated immunoglobulin-like receptor 1; PDC, pyridinium dichromate; TBAB, tetra-*n*-butylammonium bromide; TBAF, tetra-*n*-butylammonium fluoride; TBSCl, *tert*-butyldimethylsilyl chloride; TOCSY, ^1H-^1H total correlation spectroscopy; VD_3, vitamin D_3; VDR, vitamin D receptor; VDRE, vitamin D response element.

REFERENCES

1. Zhu, J. G.; Ochalek, J. T.; Kaufmann, M.; Jones, G.; Deluca, H. F. CYP2R1 is a major, but not exclusive, contributor to 25-hydroxyvitamin D production in vivo. *Proc. Natl. Acad. Sci. U. S. A.* **2013,** *110*, 15650-15655.
2. Haussler, M. R.; Whitfield, G. K.; Haussler, C. A.; Hsieh, J. C.; Thompson, P. D.; Selznick, S. H.; Dominguez, C. E.; Jurutka, P. W. The nuclear vitamin D receptor: biological and molecular regulatory properties revealed. *J. Bone Miner. Res.* **1998,** *13*, 325-349.
3. Tieu, E. W.; Tang, E. K.; Chen, J.; Li, W.; Nguyen, M. N.; Janjetovic, Z.; Slominski, A.; Tuckey, R. C. Rat CYP24A1 acts on 20-hydroxyvitamin D(3) producing hydroxylated products with increased biological activity. *Biochem. Pharmacol.* **2012,** *84*, 1696-1704.
4. Lin, Z.; Li, W. The roles of vitamin D and its analogs in inflammatory diseases. *Curr. Top. Med. Chem.* **2016,** *16*, 1-20.
5. Slominski, A.; Semak, I.; Zjawiony, J.; Wortsman, J.; Li, W.; Szczesniewski, A.; Tuckey, R. C. The cytochrome P450scc system opens an alternate pathway of vitamin D3 metabolism. *FEBS J.* **2005,** *272*, 4080-4090.
6. Tuckey, R. C.; Li, W.; Zjawiony, J. K.; Zmijewski, M. A.; Nguyen, M. N.; Sweatman, T.; Miller, D.; Slominski, A. Pathways and products for the metabolism of vitamin D3 by cytochrome P450scc. *FEBS J.* **2008,** *275*, 2585-2596.
7. Slominski, A. T.; Kim, T. K.; Shehabi, H. Z.; Semak, I.; Tang, E. K.; Nguyen, M. N.; Benson, H. A.; Korik, E.; Janjetovic, Z.; Chen, J.; Yates, C. R.; Postlethwaite, A.; Li, W.; Tuckey, R. C. In vivo evidence for a novel pathway

of vitamin D(3) metabolism initiated by P450scc and modified by CYP27B1. *FASEB J.* **2012,** *26*, 3901-3915.
8. Slominski, A. T.; Li, W.; Kim, T. K.; Semak, I.; Wang, J.; Zjawiony, J. K.; Tuckey, R. C. Novel activities of CYP11A1 and their potential physiological significance. *J. Steroid Biochem. Mol. Biol.* **2015,** *151*, 25-37.
9. Slominski, A. T.; Kim, T. K.; Li, W.; Yi, A. K.; Postlethwaite, A.; Tuckey, R. C. The role of CYP11A1 in the production of vitamin D metabolites and their role in the regulation of epidermal functions. *J. Steroid Biochem. Mol. Biol.* **2014,** *144 Pt A*, 28-39.
10. Slominski, A. T.; Kim, T. K.; Li, W.; Postlethwaite, A.; Tieu, E. W.; Tang, E. K.; Tuckey, R. C. Detection of novel CYP11A1-derived secosteroids in the human epidermis and serum and pig adrenal gland. *Sci. Rep.* **2015,** *5*, 14875.
11. Slominski, A. T.; Kim, T. K.; Janjetovic, Z.; Tuckey, R. C.; Bieniek, R.; Yue, J.; Li, W.; Chen, J.; Nguyen, M. N.; Tang, E. K.; Miller, D.; Chen, T. C.; Holick, M. 20-Hydroxyvitamin D2 is a noncalcemic analog of vitamin D with potent antiproliferative and prodifferentiation activities in normal and malignant cells. *Am. J. Physiol. Cell Physiol.* **2011,** *300*, C526-541.
12. Kim, T. K.; Wang, J.; Janjetovic, Z.; Chen, J.; Tuckey, R. C.; Nguyen, M. N.; Tang, E. K.; Miller, D.; Li, W.; Slominski, A. T. Correlation between secosteroid-induced vitamin D receptor activity in melanoma cells and computer-modeled receptor binding strength. *Mol. Cell. Endocrinol.* **2012,** *361*, 143-152.
13. Slominski, A. T.; Kim, T. K.; Takeda, Y.; Janjetovic, Z.; Brozyna, A. A.; Skobowiat, C.; Wang, J.; Postlethwaite, A.; Li, W.; Tuckey, R. C.; Jetten, A. M. RORalpha and ROR gamma are expressed in human skin and serve as receptors for endogenously produced noncalcemic 20-hydroxy- and 20,23-dihydroxyvitamin D. *FASEB J.* **2014,** *28*, 2775-2789.
14. Tuckey, R. C.; Li, W.; Shehabi, H. Z.; Janjetovic, Z.; Nguyen, M. N.; Kim, T. K.; Chen, J.; Howell, D. E.; Benson, H. A. E.; Sweatman, T.; Baldisseri, D. M.; Slominski, A. Production of 22-hydroxy metabolites of vitamin D-3 by cytochrome P450scc (CYP11A1) and analysis of their biological activities on skin cells. *Drug Metab. Dispos.* **2011,** *39*, 1577-1588.
15. Slominski, A. T.; Janjetovic, Z.; Fuller, B. E.; Zmijewski, M. A.; Tuckey, R. C.; Nguyen, M. N.; Sweatman, T.; Li, W.; Zjawiony, J.; Miller, D.; Chen, T. C.; Lozanski, G.; Holick, M. F. Products of vitamin D3 or 7-dehydrocholesterol metabolism by cytochrome P450scc show anti-leukemia effects, having low or absent calcemic activity. *PLoS One* **2010,** *5*, e9907.
16. Slominski, A. T.; Janjetovic, Z.; Kim, T. K.; Wright, A. C.; Grese, L. N.; Riney, S. J.; Nguyen, M. N.; Tuckey, R. C. Novel vitamin D hydroxyderivatives inhibit melanoma growth and show differential effects on normal melanocytes. *Anticancer Res.* **2012,** *32*, 3733-3742.
17. Janjetovic, Z.; Brozyna, A. A.; Tuckey, R. C.; Kim, T. K.; Nguyen, M. N.; Jozwicki, W.; Pfeffer, S. R.; Pfeffer, L. M.; Slominski, A. T. High basal NF-kappaB activity in nonpigmented melanoma cells is associated with an enhanced sensitivity to vitamin D3 derivatives. *Br. J. Cancer* **2011,** *105*, 1874-1884.
18. Janjetovic, Z.; Tuckey, R. C.; Nguyen, M. N.; Thorpe, E. M., Jr.; Slominski, A. T. 20,23-dihydroxyvitamin D3, novel P450scc product, stimulates differentiation and inhibits proliferation and NF-kappaB activity in human keratinocytes. *J. Cell. Physiol.* **2010,** *223*, 36-48.
19. Janjetovic, Z.; Zmijewski, M. A.; Tuckey, R. C.; DeLeon, D. A.; Nguyen, M. N.; Pfeffer, L. M.; Slominski, A. T. 20-Hydroxycholecalciferol, product of vitamin D3 hydroxylation by P450scc, decreases NF-kappaB activity by increasing IkappaB alpha levels in human keratinocytes. *PLoS One* **2009,** *4*, e5988.
20. Slominski, A.; Janjetovic, Z.; Tuckey, R. C.; Nguyen, M. N.; Bhattacharya, K. G.; Wang, J.; Li, W.; Jiao, Y.; Gu, W.; Brown, M.; Postlethwaite, A. E. 20S-hydroxyvitamin D3, noncalcemic product of CYP11A1 action on vitamin D3, exhibits potent antifibrogenic activity in vivo. *J. Clin. Endocrinol. Metab.* **2013,** *98*, E298-303.
21. Wang, Q.; Lin, Z.; Kim, T. K.; Slominski, A. T.; Miller, D. D.; Li, W. Total synthesis of biologically active 20S-hydroxyvitamin D3. *Steroids* **2015,** *104*, 153-162.
22. Chen, J.; Wang, J.; Kim, T. K.; Tieu, E. W.; Tang, E. K.; Lin, Z.; Kovacic, D.; Miller, D. D.; Postlethwaite, A.; Tuckey, R. C.; Slominski, A. T.; Li, W. Novel vitamin D analogs as potential therapeutics: metabolism, toxicity profiling, and antiproliferative activity. *Anticancer Res.* **2014,** *34*, 2153-2163.
23. Xiao, M.; Wang, J.; Lin, Z.; Lu, Y.; Li, Z.; White, S. W.; Miller, D. D.; Li, W. Design, synthesis and structure-activity relationship studies of novel survivin inhibitors with potent anti-proliferative properties. *PLoS One* **2015,** *10*, e0129807.
24. Lin, Z.; Marepally, S. R.; Ma, D.; Myers, L. K.; Postlethwaite, A. E.; Tuckey, R. C.; Cheng, C. Y.; Kim, T. K.; Yue, J.; Slominski, A. T.; Miller, D. D.; Li, W. Chemical synthesis and biological activities of 20S,24S/R-dihydroxyvitamin D3 epimers and their 1alpha-hydroxyl derivatives. *J. Med. Chem.* **2015,** *58*, 7881-7887.
25. Li, W.; Chen, J.; Janjetovic, Z.; Kim, T. K.; Sweatman, T.; Lu, Y.; Zjawiony, J.; Tuckey, R. C.; Miller, D.; Slominski, A. Chemical synthesis of 20S-hydroxyvitamin D3, which shows antiproliferative activity. *Steroids* **2010,** *75*, 926-935.
26. Lu, Y.; Chen, J.; Janjetovic, Z.; Michaels, P.; Tang, E. K.; Wang, J.; Tuckey, R. C.; Slominski, A. T.; Li, W.; Miller, D. D. Design, synthesis, and biological action of 20R-hydroxyvitamin D3. *J. Med. Chem.* **2012,** *55*, 3573-3577.
27. Tang, E. K.; Li, W.; Janjetovic, Z.; Nguyen, M. N.; Wang, Z.; Slominski, A.; Tuckey, R. C. Purified mouse CYP27B1 can hydroxylate 20,23-dihydroxyvitamin D3, producing 1alpha,20,23-trihydroxyvitamin D3, which has altered biological activity. *Drug Metab. Dispos.* **2010,** *38*, 1553-1559.
28. Lin, Z.; Yang, R.; Guan, Z.; Chen, A.; Li, W. Ultra-performance LC separation and quadrupole time-of-flight MS identification of major alkaloids in Plumula Nelumbinis. *Phytochem. Anal.* **2014,** *25*, 485-494.
29. Pingili, A. K.; Kara, M.; Khan, N. S.; Estes, A. M.; Lin, Z.; Li, W.; Gonzalez, F. J.; Malik, K. U. 6beta-hydroxytestosterone, a cytochrome P450 1B1 metabolite of testosterone, contributes to angiotensin II-induced hypertension and its pathogenesis in male mice. *Hypertension* **2015,** *65*, 1279-1287.
30. Cheng, C. Y.; Slominski, A. T.; Tuckey, R. C. Metabolism of 20-hydroxyvitamin D3 by mouse liver microsomes. *J. Steroid Biochem. Mol. Biol.* **2014,** *144 Pt B*, 286-293.
31. Tang, E. K.; Chen, J.; Janjetovic, Z.; Tieu, E. W.; Slominski, A. T.; Li, W.; Tuckey, R. C. Hydroxylation of CYP11A1-derived products of vitamin D3 metabolism by human and mouse CYP27B1. *Drug Metab. Dispos.* **2013,** *41*, 1112-1124.
32. Meyaard, L. The inhibitory collagen receptor LAIR-1 (CD305). *J. Leukoc. Biol.* **2008,** *83*, 799-803.

Table of Contents graphic